Available online at www.sciencedirect.com

ScienceDirect

Ceramics International 40 (2014) 3209–3214

CERAMICS INTERNATIONAL

www.elsevier.com/locate/ceramint

Synthesis and characterization of nanocrystalline zinc aluminate spinel powder by sol–gel method

Ravi Kant Sharma, Ranjana Ghose*

Department of Chemistry, Indian Institute of Technology (B.H.U), Varanasi 221005, India

Received 2 August 2013; received in revised form 14 September 2013; accepted 27 September 2013
Available online 8 October 2013

Abstract

Single-phase nanocrystalline zinc aluminate ($ZnAl_2O_4$) spinel powder has been synthesized by the sol–gel method. Zinc aluminate nanoparticles were formed at 600 °C, which is at much lower temperature than by solid state reactions. Formation of $ZnAl_2O_4$ and their particle size depend on the calcination temperature. Calcination temperature also affects the specific surface area and pore volume. The nanocrystalline zinc aluminate was characterized by powder X-ray diffraction, FT-IR spectroscopy, thermal gravimetric analysis, diffuse reflectance spectroscopy, surface area measurements, field emission scanning electron microscopy coupled with energy dispersive X-ray analysis and transmission electron microscopy. Catalytic reactivity of nanocrystalline zinc aluminate was tested for the reduction of 4-nitrophenol to 4-aminophenol using $NaBH_4$.

Keywords: A. Sol–gel processes; B. X-ray methods; D. Spinels; Catalytic reactivity

1. Introduction

Nanocrystalline zinc aluminate with spinel type structure is widely applied in various fields because of its interesting properties such as high mechanical strength, high thermal stability, low surface acidity, better diffusion, low temperature sintering ability, wide band-gap energy, hydrophobicity, excellent optical transparency, good metal dispersion capacity and chemical resistance [1–5]. Nanosized zinc aluminate powders and their compact crystal structure are generally used as high temperature ceramic materials, sensors, electronic materials, catalyst and catalytic support of transition metal due to their high specific surface area [6–8]. It has also been used as a heterogeneous catalyst in many reactions, such as acetylation, methylation, dehydration, hydrogenation, dehydrogenation and oxidation of benzyl alcohol to benzaldehyde [6,8–11]. Zinc aluminate nanoparticles are also good photocatalysts, e.g., in the degradation of textile dye and gaseous toluene [12,13]. Zinc aluminate ($ZnAl_2O_4$) is a typical example of normal spinel type structure having the general formula AB_2O_4, where A and B are divalent and trivalent metal ions. In this structure there are four octahedral holes and eight tetrahedral holes per molecule. In normal spinels, A^{2+} ions occupy tetrahedral holes and B^{3+} ions are present in the octahedral holes and the anions are arranged in a cubic close packed array [14].

$ZnAl_2O_4$ nanocrystalline powder has been synthesized by many methods such as microwave assisted hydrothermal [1], co-precipitation [9], hydrothermal [15], solvothermal [16], combustion [17], polymeric precursors [18], modified citrate [19], pyrolysis [20], microemulsion [21], solid state high temperature reactions [22] and evaporation-induced self assembly method [23]. These methods need sophisticated apparatus and are expensive. The major disadvantages of the high temperature, co-precipitation and other methods are that the products obtained usually possess low surface area and inhomogeneity. The significance of the sol–gel process as compared to other methods is that it includes the ability of maintaining a high degree of purity and high homogeneity. Samples are prepared at low temperatures at low cost with good control of size, structure, and morphology [5,11,14]. The sol–gel method has been used to synthesize $ZnAl_2O_4$

*Corresponding author. Tel.: +91 0542 6702879; fax: +91 5422368428.
E-mail addresses: ravikant.iitr.32@gmail.com (R.K. Sharma), rghose.apc@itbhu.ac.in (R. Ghose).

0272-8842/$ - see front matter © 2013 Elsevier Ltd and Techna Group S.r.l. All rights reserved.
http://dx.doi.org/10.1016/j.ceramint.2013.09.121

nanoparticles by several authors. Charinpanitkul et al. [2] and Wei and Chen [3] have reported the preparation of $ZnAl_2O_4$ nanoparticles using ethylacetoacetate and oxalic acid as the chelating agent respectively. In the present work, very pure $ZnAl_2O_4$ nanoparticles have been synthesized without using any chelating agent.

2. Experimental

Aluminium isopropoxide (98%, ALDRICH®), zinc acetate (SRL®), toluene (RANKEM®), ammonia solution (25%, RANKEM®)), 4-nitrophenol (SRL®), $NaBH_4$ (HIMEDIA®), ethanol (MERCK®), and Millipore® water were used as the reagents as received. In the present study, $ZnAl_2O_4$ nanoparticles were synthesized using suitable precursors by the sol–gel method [24]. The details of procedure are as follows.

Zinc acetate: Aluminium isopropoxide (1:2 M ratio), 100 mL of toluene, 40 mL of ethanol and 0.5 mL water (Millipore®) were taken in a 250 mL round bottom flask. The contents were vigorously stirred for 3 h at room temperature till the mixture became homogenous. Then, 2 mL of 25% ammonia solution was added followed by the addition of about 1 mL of water after 1 h. The contents were kept for constant stirring for about 24 h at room temperature (25 °C). The obtained slurry was evaporated at 80 °C to form a gel. The gel was dried at ~80 °C for a few hours and then ground to obtain the xerogel powder. Then the as-prepared powder was calcined in air at 500°, 600° and 700 °C for 3 h inside a muffle furnace (Nabertherm®) to obtain $ZnAl_2O_4$ powder.

Powder XRD patterns were recorded using a Brucker AXS D8 diffractometer operating with Cu-Kα radiation ($\lambda = 0.15406$ nm) with a scanning speed of 2°/min. Thermal gravimetric measurements were carried out in the temperature range 25–1000 °C using a Perkin Elmer (Pyris Diamond) instrument in nitrogen atmosphere at a heating rate of 5°/min. A Thermo Nicolet Nexus Fourier FT-IR spectrophotometer in the range 4000–400 cm^{-1} was used for recording IR spectra of the nanocrystalline powder using KBr disk method. Diffuse reflectance spectra were recorded using a Shimadzu UV-2450 UV-visible spectrophotometer attached with a diffuse reflectance accessory in the wavelength range 200–800 nm using $BaSO_4$ as the reference. The specific surface area of the nanocrystalline powder was measured using Brunauer–Emmett–Teller (BET) method by Micromeritics Chemisorb 2720 instrument using nitrogen physisorption. Morphology of the samples along with elemental analysis (EDXA) data were obtained with a field emission scanning electron microscope (FE-SEM) using FEI Quanta 200 F operating at an accelerating voltage of 20 kV. TEM images of the nanocrystalline powder were recorded using a FEI TECNAI G2 electron microscope operating at an accelerating voltage of 200 kV. The nanocrystalline zinc aluminate powder was dispersed in ethanol using low power sonicator and putting a drop over carbon coated copper grid followed by drying for the TEM measurements.

The catalytic reactivity of the synthesized nanocrystalline zinc aluminate powder was tested by carrying out the conversion of 4-nitrophenol to 4-aminophenol using $NaBH_4$ as the reducing agent at room temperature [20]. This reaction has also been used to find the catalytic activity of different metal aluminate nanoparticles [20,24]. Approximately 50 mL aqueous solution of 4-nitrophenol (0.1 mmol) and 50 mL of freshly prepared aqueous solution of $NaBH_4$ (0.53 mol/L) were taken in a 250 mL beaker. Then, 18.3 mg of the catalyst (zinc aluminate nanoparticles) was added to the above mixture with constant stirring at room temperature. Complete reduction of 4-nitrophenol (yellow colored solution) to 4-aminophenol was indicated by decolorization of the solution and the time taken for the decolorization was noted.

3. Results and discussion

The powder XRD patterns of as-prepared and calcined zinc aluminate powder samples are shown in Fig. 1. The as-prepared sample is X-ray amorphous. It is observed that with increasing temperature crystallinity of the particles increases and also the intensity of the diffraction peaks increases showing that the particle size becomes larger. The powder sample, when calcined at 700 °C gives high intensity fine peaks. The calcined samples show peaks at $2\theta \approx 31.36°$, 36.73°, 44.85°, 49.09°, 55.77°, 59.52°, 65.39°, 74.19°, and 77.35° which are indexed as (220), (311), (400), (331), (422), (511), (440), (620), and (533) diffraction lines showing cubic crystalline zinc aluminate spinel type structure (JCPDS file no. 05-0669). The XRD patterns confirm that the material obtained in the present work is of very high purity with single-phase. The crystallite size of pure nanocrystalline zinc aluminate was calculated using the Debye–Scherrer formula as given below [25].

$$\delta = 0.89\lambda/\beta \cos \theta \quad (1)$$

Where δ is the crystallite size in nm. 0.89 represents a dimensionless constant k, λ is the wavelength of Cu-Kα (0.15406 nm), β is full width at half maxima and θ is the angle. The crystallite size calculated using the most intense peak (311) at $2\theta \approx 36.73°$ of nanocrystalline zinc aluminate calcined at 500° C, 600° C and 700 °C was 3.85 nm, 13.24 nm and 16.80 nm, respectively.

The thermal gravimetric analysis patterns for as-prepared powder show three steps of weight loss (Fig. 2). The first

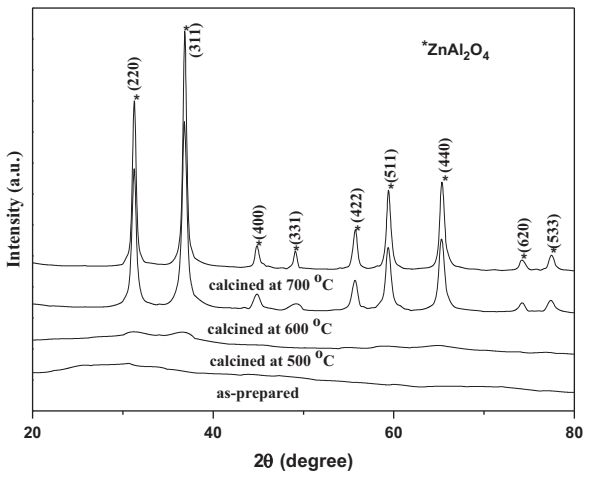

Fig. 1. XRD patterns of nanocrystalline zinc aluminate (before and after calcination).

weight loss step (9%) observed in the temperature range from 50–132 °C is mainly attributed to the physically adsorbed water molecules. The second weight loss (about 15 mass %) in the region 132–350 °C is due to the removal of organic impurities from the precursors [6].The third weight loss step in the region 350–500 °C is due to the decomposition of anhydrous Zn $(OH)_2$ $2Al(OH)_3$ to $ZnAl_2O_4$ [9].There is no weight loss after 500 °C, confirming the formation of $ZnAl_2O_4$ spinel.

The FT-IR spectra of as-prepared and calcined zinc aluminates show small peaks at about 2976 and 2876 cm^{-1} which attribute to C–H stretching (Fig. 3) [14]. The bands at 1727 and 1618 cm^{-1} are assigned to the free carboxyl groups [14] and to the bending vibrational mode of water molecules [16] respectively. The weak bands observed between 1572 and 1372 cm^{-1} exhibit the presence of organic compounds [16]. The bands observed between 1000–1100 cm^{-1} are assigned to the C–O and C–C vibrations [26]. In zinc aluminate spinel powder, metal–oxygen stretching frequencies appear in the range 500–900 cm^{-1}, which are associated with the vibrations of Zn–O, Al–O, and Zn–O–Al bands [13,27].

Diffuse reflectance spectra of nanocrystalline zinc aluminate before and after calcination at different temperatures are shown in Fig. 4. The UV-visible spectra of as-prepared as well as calcined nanocrystalline zinc aluminate exhibit characteristic broad absorption band corresponding to $ZnAl_2O_4$ spinel [11]. Surface area measurements (BET) were carried out for nanocrystalline zinc aluminate before and after calcination (Table 1). The results indicate that as-prepared zinc aluminate sample has high specific surface area (SSA ~ 332.4 $m^2 g^{-1}$) and total pore volume (TPV ~ 0.21 $cm^3 g^{-1}$) compared to the calcined nanocrystalline zinc aluminate spinel (500 °C: SSA ~ 195.3 $m^2 g^{-1}$, TPV ~ 0.19 $cm^3 g^{-1}$, 600 °C: SSA ~ 146.5 $m^2 g^{-1}$, TPV ~ 0.17 $cm^3 g^{-1}$ and 700 °C: SSA ~ 129.2 $m^2 g^{-1}$, TPV ~ 0.14 $cm^3 g^{-1}$). Thus, $ZnAl_2O_4$ spinel powder obtained in the present synthesis method has higher surface area (given above) compared to the earlier reported methods. The specific surface area of $ZnAl_2O_4$ spinel synthesized by the combustion [7], co-precipitation [9] and evaporation-induced self assembly [23] methods are about 15 $m^2 g^{-1}$, 86 $m^2 g^{-1}$ and 108 $m^2 g^{-1}$, respectively.

The FE-SEM images of the nanocrystalline zinc aluminate (before and after calcination) show agglomeration of particles with irregular morphology (Fig. 5(a)–(c)). The EDX analysis

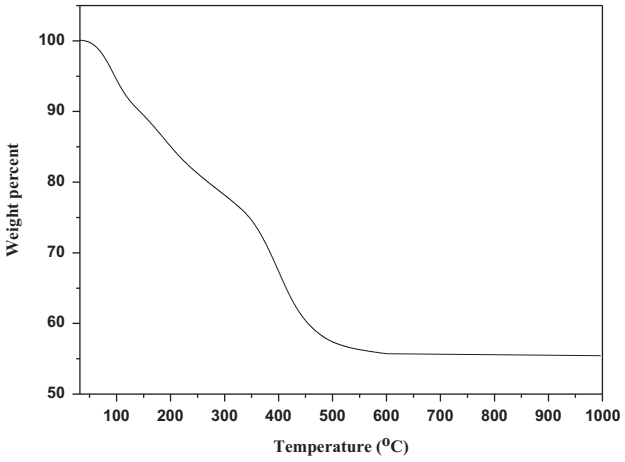

Fig. 2. Thermal gravimetric analysis curves of nanocrystalline zinc aluminate.

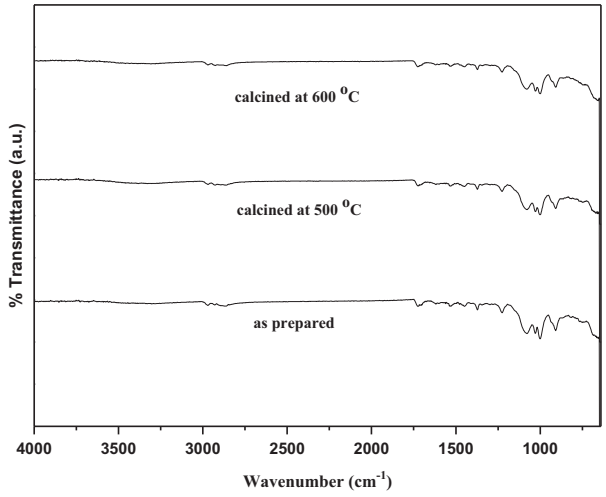

Fig. 3. FT-IR spectra of nanocrystalline zinc aluminate (before and after calcination).

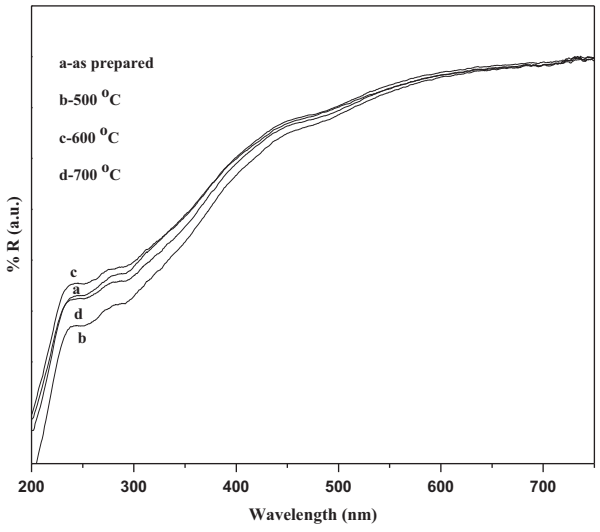

Fig. 4. Diffuse reflectance spectra of nanocrystalline zinc aluminate (before and after calcination).

Table 1
BET surface area and pore volume of nanocrystalline zinc aluminate before and after calcination.

Sample	Surface area ($m^2 g^{-1}$)	Pore volume ($cm^3 g^{-1}$)
$ZnAl_2O_4$ (before calcination)	332.4	0.21
$ZnAl_2O_4$ (calcined at 500 °C)	195.3	0.19
$ZnAl_2O_4$ (calcined at 600 °C)	146.5	0.17
$ZnAl_2O_4$ (calcined at 700 °C)	129.2	0.14

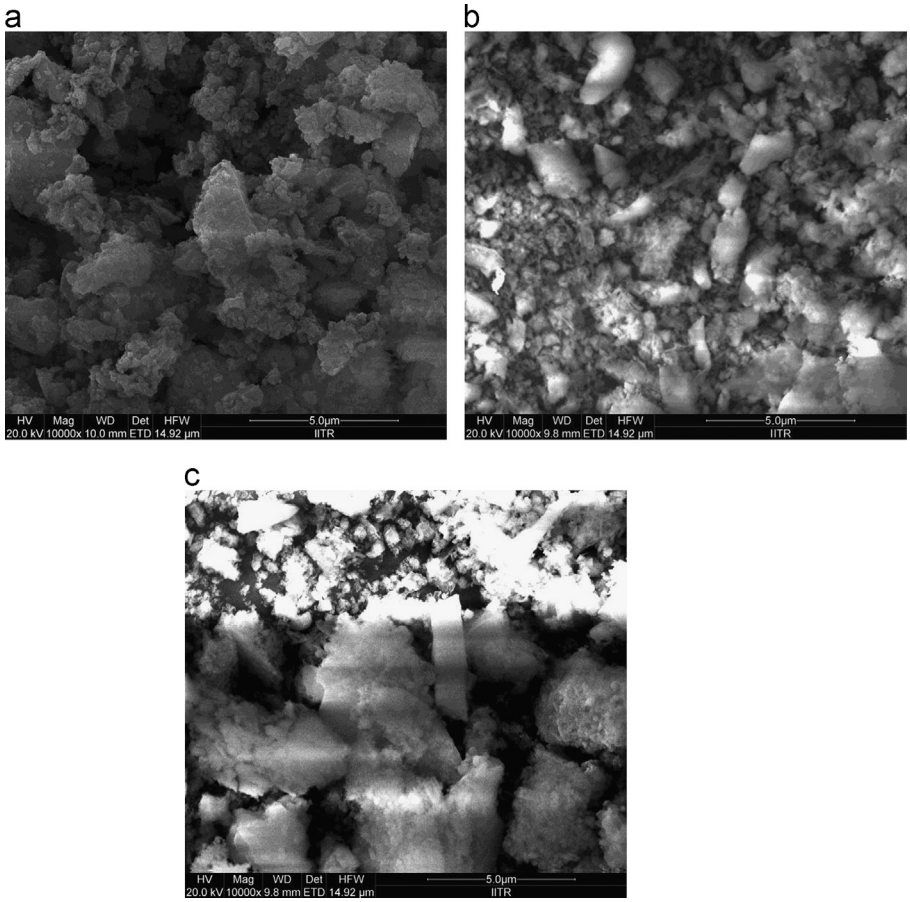

Fig. 5. SEM images of nanocrystalline zinc aluminate (a) before calcination, (b) calcined at 500 °C and (c) 600 °C.

Table 2
EDXA data of nanocrystalline zinc aluminate before and after calcination.

Element		At%	Wt%	Zn:Al
Nanocrystalline $ZnAl_2O_4$ before calcination	Zn	3.63	13.46	1:3
	Al	10.94	16.46	
Nanocrystalline $ZnAl_2O_4$ calcined at 500 °C	Zn	4.82	17.23	1.20:3.40
	Al	13.45	19.84	
Nanocrystalline $ZnAl_2O_4$ calcined at 700 °C	Zn	4.40	16.08	1.20:3.40
	Al	12.26	18.52	

results indicate the presence of zinc, aluminium and oxygen elements in the nanocrystalline zinc aluminate powder. The atomic ratio of zinc to aluminium for the nanocrystalline zinc aluminate of as-prepared sample (i.e. at% of Zn to Al = 1:3) and calcined samples at 500° C and 700 °C (i.e. at% of Zn to Al = 1.20:3.40) is calculated by EDX analysis data (Tables 2 and 3). The EDX analysis data indicate almost uniform distribution of zinc, aluminium and oxygen elements through the whole nanocrystalline zinc aluminate structure. Typical TEM images for the nanocrystalline zinc aluminate powder obtained by calcination at 500° C and 600 °C are shown in Figs. 6(a) and (b). The TEM images indicate that the zinc aluminate nanoparticles are close to spherical morphology with a fairly uniform distribution. The average particle size obtained from TEM images of nanocrystalline zinc aluminate calcined at 500° C and 600 °C are 6.25 ± 1.25 nm and 14.2 ± 0.96 nm, respectively. It is observed that the agglomeration of particles increases with increasing temperature.

The catalytic reactivity of the nanocrystalline zinc aluminate powder was studied using the reduction of 4-nitrophenol to 4-aminophenol by $NaBH_4$. The reduction of 4-nitrophenol with $NaBH_4$ was also carried out without the catalyst. The time required, for the complete conversion of 4-nitrophenol to 4-aminophenol, as observed by the decolorization of yellow color of 4-nitrophenol in the presence of synthesized powders, are summarized in Table 3. From the Table 3, it is inferred that the reduction of 4-nitrophenol does not take place in the absence of the catalyst. In addition, the reduction of 4-nitrophenol does not take place when pure alumina nanoparticles are used as catalyst. The mechanism [24] for catalysis is that first the adsorption of 4-nitrophenol as well as BH_4^- ions take place on the surface of the nanocrystalline zinc aluminate powder. After that, zinc aluminate nanoparticles help in the transfer of electrons from donor BH_4^- ions to the acceptor NO_2 group and the formation of 4-aminophenolate ions take place which then get desorbed from the surface of the catalyst. The nanocrystalline zinc aluminate powder acts as a better catalyst for the reduction of 4-nitrophenol (time of reduction: 15 min) as compared to the reported results (time of reduction: 22 min) by Dhak and pramanik [20].

Table 3
Time required for the complete reduction of 4-nitrophenol in the presence of nanocrystalline zinc aluminate as catalysts.

Sl. no.	Reaction condition	Time required for the reduction (min)
1.	4-nitrophenol + $NaBH_4$	No reduction
2.	4-nitrophenol + $NaBH_4$ + Alumina nanoparticles	No reduction
3.	4-nitrophenol + $NaBH_4$ + Nanocrystalline $ZnAl_2O_4$	15

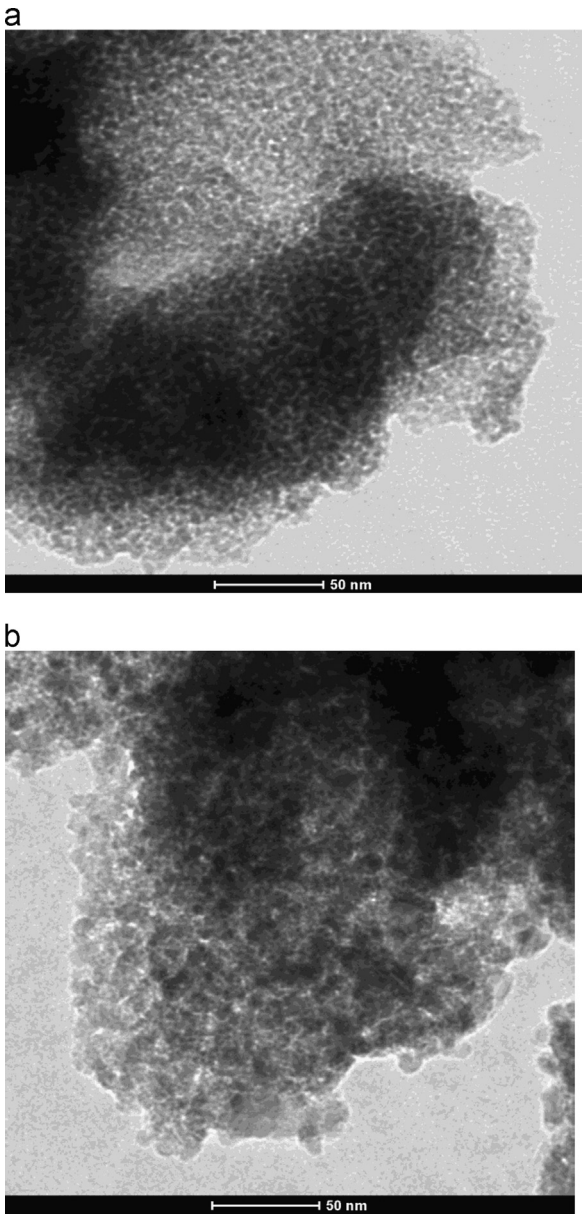

Fig. 6. TEM images of nanocrystalline zinc aluminate (a) calcined at 500 °C and (b) 600 °C.

4. Conclusions

Single-phase nanocrystalline zinc aluminate powder was successfully synthesized by simple sol–gel method without using any chelating agent. The nanocrystalline powder was characterized using various analytical techniques. The calcination temperature is an important factor for the formation of nanocrystalline $ZnAl_2O_4$ spinel powder. It affects their particle size, specific surface area, pore volume and surface morphology. Surface area measurements indicate that nanocrystalline zinc aluminate obtained under the sol–gel method has high surface area. Catalytic activity of the nanocrystalline zinc aluminate powder was tested for the reduction of 4-nitrophenol to 4-aminophenol. The studies indicate that the present nanocrystalline powder acts as a better catalyst compared to earlier reported work.

Acknowledgment

Ravi Kant Sharma would like to thank the Ministry of Human Resource and Development, Government of India, for providing financial support during the research work. We are thankful to Professor U.P Singh, Department of Chemistry, IIT, Roorkee for helping in carrying out the present work. Thanks extended also to the Institute Instrumentation centre, IIT, Roorkee for providing the facilities.

References

[1] M. Zawadzki, Synthesis of nanosized and microporous zinc aluminate spinel by microwave assisted hydrothermal method, Solid State Sciences 8 (2006) 14–18.
[2] T. Charinpanitkul, P. Poommarin, A. Wongkaew, K.S. Kim, Dependence of zinc aluminate microscopic structure on its synthesis, Journal of Industrial and Engineering Chemistry 15 (2009) 163–166.
[3] X. Wei, D. Chen, Synthesis and characterization of nanosized zinc aluminate spinel by sol–gel technique, Materials Letters 60 (2006) 823–827.
[4] M. Zawadzki, W. Staszak, F.E.L. Suarez, M.J.I. Gomez, A.B. Lopez, Preparation, characterisation and catalytic performance for soot oxidation of copper-containing $ZnAl_2O_4$ spinels, Applied Catalysis A: General 371 (2009) 92–98.
[5] X. Duan, D. Yuan, X. Wang, H. Xu, Synthesis and characterization of nanocrystalline zinc aluminum spinel by a new sol–gel method, Journal of Sol–Gel Science and Technology 35 (2005) 221–224.
[6] D.L. Ge, Y.J. Fan, C.L. Qi, Z.X. Sun, Facile synthesis of highly thermostable mesoporous $ZnAl_2O_4$ with adjustable pore size, Journal of Materials Chemistry A 1 (2013) 1651–1658.
[7] C.T. Alves, A. Oliveira, S.A.V. Carneiro, A.G. Silva, H.M.C. Andrade, S. A.B. Vieira de Melo, E.A. Torres, Transesterification of waste frying oil using a zinc aluminate catalyst, Fuel Processing Technology 106 (2013) 102–107.
[8] G. Fan, J. Wang, F. Li, Synthesis of high-surface-area micro/mesoporous $ZnAl_2O_4$ catalyst support and application in selective hydrogenation of o-chloronitrobenzene, Catalysis Communications 15 (2011) 113–117.
[9] S. Farhadi, S. Panahandehjoo, Spinel-type zinc aluminate ($ZnAl_2O_4$) nanoparticles prepared by the co-precipitation method: a novel, green and recyclable heterogeneous catalyst for the acetylation of amines, alcohols and phenols under solvent-free conditions, Applied Catalysis A: General 382 (2010) 293–302.
[10] M. Ranjbar, M.S. Niasari, S.M.H. Mashkani, Microwave synthesis and characterization of spinel-type zinc aluminate nanoparticles, Journal of Inorganic and Organometallic Polymers 22 (2012) 1093–1100.
[11] R.T. Kumar, N.C.S. Selvam, C. Ragupathi, L.J. Kennedy, J.J. Vijaya, Synthesis, characterization and performance of porous Sr (II)-added $ZnAl_2O_4$ nanomaterials for optical and catalytic applications, Powder Technology 224 (2012) 147–154.

[12] E.L. Foletto, S. Battiston, J.M. Simoes, M.M. Bassaco, L.S.F. Pereira, E. M. de Moraes Flores, E.I. Muller, Synthesis of $ZnAl_2O_4$ nanoparticles by different routes and the effect of its pore size on the photocatalytic process, Microporous and Mesoporous Materials 163 (2012) 29–33.
[13] X. Li, Z. Zhu, Q. Zhao, L. Wang, Photocatalytic degradation of gaseous toluene over $ZnAl_2O_4$ prepared by different methods: a comparative study, Journal of Hazardous Materials 186 (2011) 2089–2096.
[14] A.G. Khaledi, S. Afshar, H.S. Jahromi, Improving $ZnAl_2O_4$ structure by using chelating agents, Materials Chemistry and Physics 135 (2012) 855–862.
[15] C.C. Yang, S.Y. Chen, S.Y. Cheng, Synthesis and physical characteristics of $ZnAl_2O_4$ nanocrystalline and $ZnAl_2O_4$/Eu core–shell structure via hydrothermal route, Powder Technology 148 (2004) 3–6.
[16] W. Staszak, M. Zawadzki, J. Okal, Solvothermal synthesis and characterization of nanosized zinc aluminate spinel used in iso-butane combustion, Journal of Alloys and Compounds 492 (2010) 500–507.
[17] R. Ianos, R. Lazau, I. Lazau, C. Pacurariu, Chemical oxidation of residual carbon from $ZnAl_2O_4$ powders prepared by combustion synthesis, Journal of the European Ceramic Society 32 (2012) 1605–1611.
[18] L. Gama, M.A. Ribeiro, B.S. Barros, R.H.A. Kiminami, I.T. Weber, A.C. F.M. Costa, Synthesis and characterization of the $NiAl_2O_4$, $CoAl_2O_4$ and $ZnAl_2O_4$ spinels by the polymeric precursors method, Journal of Alloys and Compounds 483 (2009) 453–455.
[19] L. Chen, X. Sun, Y. Liu, K. Zhou, Y. Li, Porous $ZnAl_2O_4$ synthesized by a modified citrate technique, Journal of Alloys and Compounds 376 (2004) 257–261.
[20] D. Dhak, P. Pramanik, Particle size comparison of soft-chemically prepared transition metal (Co, Ni, Cu, Zn) aluminate spinels, Journal of the American Ceramic Society 89 (2006) 1014–1021.
[21] V. Ciupina, I. Carazeanu, G. Prodan, Characterization of $ZnAl_2O_4$ nanocrystals prepared by coprecipitation and microemulsion techniques, Journal of Optoelectronics and Advanced Materials 6 (2004) 1317–1322.
[22] N.J.V. Laag, M.D. Snel, P.C.M.M. Magusin, G. de With, Structural, elastic, thermophysical and dielectric properties of zinc aluminate ($ZnAl_2O_4$), Journal of the European Ceramic Society 24 (2004) 2417–2424.
[23] X. Tian, L. Wan, K. Pan, C. Tian, H. Fu, K. Shi, Facile synthesis of mesoporous $ZnAl_2O_4$ thin films through the evaporation-induced self-assembly method, Journal of Alloys and Compounds 488 (2009) 320–324.
[24] N. Bayal, P. Jeevanandam, Synthesis of metal aluminate nanoparticles by sol–gel method and studies on their reactivity, Journal of Alloys and Compounds 516 (2012) 27–32.
[25] B.D. Cullity, S.R. Stock, Elements of X-ray Diffraction, Prentice Hall, 2001.
[26] D. Visinescu, C. Paraschiv, A. Ianculescu, B. Jurca, B. Vasile, O. Carp, The environmentally benign synthesis of nanosized $Co_xZn_{1-x}Al_2O_4$ blue pigments, Dyes and Pigments 87 (2010) 125–131.
[27] Z. Zhu, X. Li, Q. Zhao, S. Liu, X. Hu, G. Chen, Facile solution synthesis and characterization of porous cubic-shaped superstructure of $ZnAl_2O_4$, Materials Letters 65 (2011) 194–197.